

SCIENTIFIC PAPERS  
OF THE UNIVERSITY OF PARDUBICE  
Series A  
Faculty of Chemical Technology  
23 (2017)

**A ZWITTERIONIC (POLY)METHACRYLATE  
MONOLITHIC CAPILLARY COLUMN WITH DUAL  
HILIC – REVERSED-PHASE MECHANISM FOR UNI-  
AND TWO-DIMENSIONAL HPLC**

Magda STAŇKOVÁ and Pavel JANDERA<sup>1</sup>  
Department of Analytical Chemistry,  
The University of Pardubice, CZ–532 10 Pardubice

Received June 6, 2016

*Sulfobetaine zwitterionic monolithic columns were synthesized by in-situ polymerization (in fused silica capillaries) of a N,N-dimethyl-N-metacryloxyethyl-N-(3-sulfopropyl) ammonium betaine (MEDSA) functional monomer in combination with different cross-linking monomers. From among the ten cross-linkers tested, bisphenol A glycerolate dimethacrylate provides monolithic capillary columns with best chromatographic efficiency (60 000-70 000 theoretical plates per meter). The respective columns show excellent column-to-column reproducibility of pore morphology, separation selectivity, good permeability and low mass transfer resistance, so that being suitable for fast and selective separation of various samples. Monolithic sulfobetaine polymethacrylate (BIGDMA-MEDSA) micro-columns designed in our laboratory exhibit a dual retention mechanism, in acetonitrile-rich mobile phase, polar (hydrophilic)*

---

<sup>1</sup> To whom correspondence should be addressed.

*interactions control the retention (HILIC separation mode), whereas in more aqueous mobile phases the column shows essentially non-polar with a major role of hydrophobic interactions properties (reversed-phase, RP mode). The dual-mode retention mechanism was investigated and applied to the HILIC and reversed-phase HPLC separations of barbiturates, sulfonamides, nucleobases, nucleosides, phenolic, and other carboxylic acids, polyphenols, flavonoids plus other low-molecular compounds. The separation selectivities in the HILIC and RP dimensions are highly complementary to each other, so that a zwitterionic sulfobetaine polymethacrylate micro-column can be used in the first dimension of two-dimensional LC in alternating RP and HILIC modes, coupled with a short (3-5 cm) alkyl-bonded core-shell or silica-based monolithic column in the second dimension, for HILIC×RP and RP×RP comprehensive two-dimensional separations. During the HILIC×RP period, a programme with the decreasing acetonitrile gradient is used for separation in the first dimension, so that at the end of the gradient the polymeric monolithic micro-column is equilibrated with a highly aqueous mobile phase and is ready for repeated sample injection, in this case, for separation under reversed-phase gradient conditions with the increasing concentration of acetonitrile in the first dimension.*

## **Introduction**

Monolithic columns are being prepared as a single-piece of highly porous material, thus providing high permeability and faster separations than particulate materials, under the moderate operational pressures. There are two main types of monoliths — (i) silica-based and (ii) polymer monolithic materials [1]. Chemically bonded silica monoliths allow one fast separations of low-molecular samples with the column efficiencies up to 100 000 theoretical plates  $m^{-1}$  [2].

Organic polymer monolithic columns were first devised by Hjertén *et al.* [3] and further developed throughout the early 1990s [4]. Porous polymer rods based on polystyrene-, polymethacrylate-, polyacrylamide-, and other matrices have come to include sophisticated column designs for columns and microfluidic devices, with various surface chemistry and/ or different concentrations of the surface functionalities [5,6]. Thin monolithic disks or rod columns are widely employed for isolation, purification, and pre-treatment of samples containing proteins, peptides or the fragments of nucleic acid.

The polymer-based monoliths offers a heterogeneous structure, which resembles a net of interconnected non-porous cauliflower-like microglobules with significantly lowered surface area. This morphology is suitable for separation of polymers requiring large pores (15-100 nm) with relatively low specific surface area ( $10-15 m^2 g^{-1}$ ) [7]. The small pores in the microglobules of organic monoliths are generally inaccessible for large molecules of biopolymers not participating in

a slow diffusion that may decrease the separation efficiency. This was the reason why, in the past, organic monoliths have traditionally shown low efficiency for the separation of small molecules [1]. Besides the low proportion of small pores and resulting low surface area, inadequate “gel porosity” of the monoliths swollen in the mobile phase was blamed for poor separation performance for low-molecular compounds [8].

Broad chemical variability, high temperature, and chemical stability of organic polymer monoliths stimulated the on-going efforts in tailored preparations of polymer-based highly efficient monolithic stationary phase suitable for the fast and efficient analysis of low molecular weight compounds. Significant progress has recently been achieved in the preparation of organic polymer monoliths with the improved separation efficiency up to 70 000-80 000 plates  $m^{-1}$  for small molecules. Various strategies were adopted to adjust the pore morphology and to improve the mass transfer in the organic polymer monoliths: 1) adjusting initiation conditions and temperature of polymerization, 2) employing a short time of the polymerization reaction allowing only partial polymerization, 3) careful optimization of the chemistry and proportions of functional monomers, cross-linkers, and porogen solvents in the polymerization mixture, 4) post-polymerization monolith modifications, or 5) incorporating additional structural elements into the monolithic skeleton, such as carbon nanotubes [1,9,10,11].

Recently, we investigated systematically the effects of the components of polymerization mixture on the pore distribution, permeability, and separation efficiency of capillary monolithic polymethacrylate columns. We prepared a series of columns using a lauryl methacrylate functional monomer and ten alkylene and oxyethylene cross-linkers, differing in the length and polarity. Monolithic columns prepared with polar tetraoxyethylene dimethacrylate (TeEDMA) cross-linker had shown the efficiency of approx. 70 000 theoretical plates  $m^{-1}$ , low mass transfer resistance, allowing thus fast separations of low-molecular compounds in 2 min or even less with the excellent column-to-column reproducibility [12].

## Theory

Reversed-phase HPLC on silica materials with bonded alkyl non-polar stationary phases is used in contemporary HPLC. However, many polar compounds exhibit too low retention and selectivity for successful separations. Hydrophilic interaction chromatography (HILIC) is becoming a very popular alternative to reversed-phase liquid chromatography for separations of polar, weakly acidic or basic samples [13]. In the HILIC separation mode, a polar stationary phase is being used in combination with aqueous-organic mobile phases containing high concentrations of organic solvent (acetonitrile) for separations of peptides, proteins, oligosaccharides, drugs, metabolites, and various natural compounds

when using a variety of polar columns, including the bare silica gel, hydrosilated silica, silica-based amino-, amido-, cyano-, carbamate-, diol-, polyol-, zwitterionic sulfobetaine, or poly(2-sulphoethyl aspartamide) and other polar stationary phases chemically bonded onto the silica gel support, but also ion-exchangers or zwitterionic materials, showing combined HILIC–ion interaction retention mechanism [14]. For instance, a zwitterionic phase bonded on a monolithic silica capillary column was used for separation of nucleic acid bases, nucleosides, and deoxynucleosides [15].

Except for electrochromatography [16-19], polar organic polymer monolithic columns have less often been employed for separations in the HILIC mode. However, almost 40 years ago, hydrophilic gel particles of a macroporous co-polymer of 2-hydroxyethyl methacrylate with ethanediol dimethacrylate and ion-exchangers produced by their modification were introduced as column packings for gel-permeation, affinity, ion exchange, and reversed-phase chromatography of polar polymers and small molecules, such as nucleosides and nucleic bases [20], barbiturates, sulfonamides [21], or phenolic compounds [22]. Structurally similar polymethacrylate monolithic based columns were later found suitable for some HILIC separations. Polymerization of glycidyl methacrylate and ethylene dimethacrylate with subsequent hydrolysis of the oxirane group, yielded a polymeric monolithic diol phase suitable for HILIC separations [16]. A monolithic (poly)hydroxymethacrylate capillary column was employed for HILIC of oligonucleotides [23].

A 0.2 mm i.d. capillary column, prepared by co-polymerization of MEDSA with 1,2-bis(p-vinylphenyl ethane (BVPE) was employed for separation of nucleic bases [24]. More frequently, zwitterionic groups are incorporated into poly(methacrylate) structures. Poly(methacrylate) monolithic columns prepared by photo-initiated co-polymerization of MEDSA and ethylene dimethacrylate (EDMA) cross-linker, and initially intended for cation-exchange separation of proteins [25, 26]. Later, Jiang *et al.* [27] prepared a hydrophilic monolithic column from the same monomers, by thermally initiated co-polymerization inside a 100- $\mu\text{m}$  i.d. fused-silica capillary, suitable for HILIC separations of neutral, basic, and acidic polar analytes in aqueous-organic mobile phases with 60% or more acetonitrile, and having been reported to offer a very good separation selectivity in comparison to particle-packed zwitterionic columns. Viklund *et al.* [26] prepared monolithic capillary columns for cation exchange LC of proteins by co-polymerization of ethylene dimethacrylate (EDMA) and N,N-dimethyl-N-methacryloxyethyl- N-(3-sulfopropyl)ammonium betaine (MEDSA) inside fused silica capillaries. Such columns were suitable for HILIC separations of neutral, basic, and acidic polar compounds in the aqueous–organic mobile phases [27]. Porosity, permeability, selectivity, and retention characteristics of monolithic sulfobetaine columns depend on the concentration of MEDSA, and on the composition of the water-containing porogen solvents in the polymerization

mixture [28]. Zwitterionic organic-silica hybrid monolithic capillary columns were used for efficient HILIC separations of various low-molecular weight neutral, basic, and acidic compounds [29].

In general, the dimethacrylate cross-linkers with longer and more polar (poly) oxyethylene groups improve the performance of polar monolithic columns intended for HILIC applications. Best results were obtained with sulfobetaine (*N,N*-dimethyl-*N*-methacryloxyethyl-*N*-(3-sulfopropyl) ammonium betaine - (MEDSA) monomer cross-linked with bisphenol A glycerolate dimethacrylate — (BIGDMA) (Fig. 1) that provided stable and reproducible polymethacrylate monolithic columns in the capillary format with efficiencies up to 70 000 theoretical plates  $m^{-1}$  [30]. The capillary BIGDMA-MEDSA monolithic columns probably contain well solvated pores, enabling fast diffusion of the sample molecules, and a low band dispersion and could thus be successfully used in the first dimension of two-dimensional HILICxRP separations of polyphenolic compounds [31]. We found that this type of columns provides a dual retention mechanism in the aqueous-organic mobile phases, HILIC at high concentrations of acetonitrile and reversed-phase (RP) in water rich mobile phases.

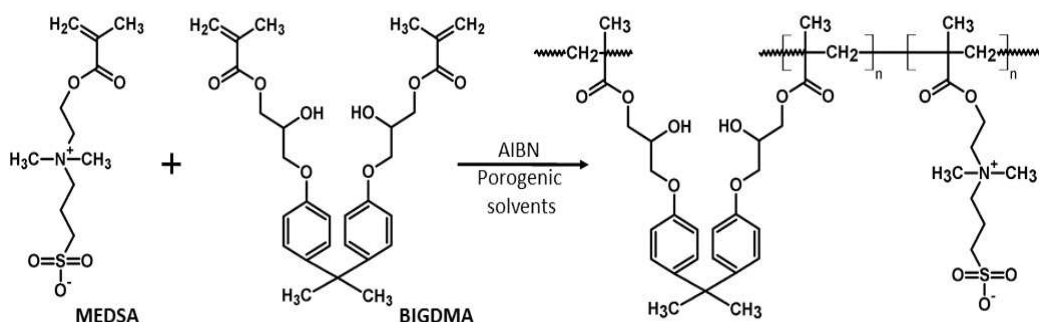


Fig.1 Scheme of co-polymerization reaction of BIGDMA and MEDSA monomers. Functional monomer MEDSA (*N,N*-dimethyl-*N*-methacryloxyethyl-*N*-(3-sulfopropyl) ammonium betaine), crosslinking monomer BIGDMA (bisphenol A glycerolate dimethacrylate)

The sulfoalkylbetaine-based phases strongly attach water by hydrogen bonding to form an adsorbed diffuse stationary phase liquid layer, besides the bulk mobile phase being much richer in the organic solvent (usually, acetonitrile). The retention mechanism is believed to involve partitioning between the bulk mobile phase and the adsorbed water layer in the stationary phase, in addition to direct adsorption on zwitterionic functionalities due mainly to polar (hydrogen-bonding and dipole-dipole) interactions, even though weak electrostatic interactions may also affect the retention of partly ionized analytes. The pH value, the concentrations of acetonitrile and the salt additive can be adjusted to control the retention and chromatographic selectivity accordingly to some particular separations.

In reversed-phase systems with binary aqueous-organic mobile phases, the retention decreases as the concentration (volume fraction),  $\varphi$ , of the organic solvent in the mobile phase increases, which is described by a widely used semi-empirical Eq. (1) valid in many RP systems; at least, over a limited mobile phase composition range [32,33].

$$\log k = \log k_0 - m_1 \varphi = a - m_1 \varphi \quad (1)$$

In aqueous-organic normal-phase systems, where localized adsorption controls the retention due to the competition or displacement Eq. (2) was assumed to describe satisfactorily the retention outside the range of very low concentrations of water [34]

$$\log k = \log k_B - m_2 \log \varphi = a' - m_2 \log \varphi \quad (2)$$

Here,  $\varphi$  is the volume fraction of water in the aqueous / organic mobile phase. The constants  $k_0$ ,  $k_B$ ,  $a$ ,  $a'$ ,  $m_1$ ,  $m_2$  in Eqs (1) and (2) depend on the solute and the type of organic solvent.

On some polar chemically bonded phases, the dual retention mechanism, involving solvophobic interactions and polar interactions with the residual silanol groups, was observed for polar compounds, with a retention minimum at the  $\log k - \varphi_{H_2O}$  plots with the “U turn” composition of the aqueous-organic mobile phase, which corresponds to the transition from the RP (at high water concentrations) into the NP (HILIC) mechanism (at high organic solvent concentrations) [34]. Similar U-turn retention behavior was also observed for some columns packed with organic polymethacrylate polymer particles — see, e.g., ref. [20].

In the presence of a dual (HILIC and RP) mechanism, Eq. (1) and Eq. (2) can be combined to describe the effects of the concentration of water,  $\varphi_{H_2O}$ , as the polar solvent on the retention factors,  $k$ , over a broad composition range of aqueous-organic mobile phases (at  $\varphi_{H_2O} > 0.02$ ). The addition of an empirical term,  $b$ , considerably improves the description of the retention over a broad retention range [28]

$$\log k = a_1 + m_{RP} \varphi_{H_2O} - m_{HILIC} \log(1 + b \varphi_{H_2O}) \quad (3)$$

Equation (3) can then describe the U-turn shape of the experimental plots of  $k$  versus the volume fraction of water in the mobile phase. The HILIC mechanism is transformed into the RP mechanism retention at the “U-turn” transition point corresponding to the minimum retention at the  $\varphi_{min}$  concentration of water in the mobile phase

$$\varphi_{\min} = \frac{m_{\text{HILIC}}}{m_{\text{RP}}} \quad (4)$$

The “U turn” mobile phase composition generally depends on the polarity of sample and on the type of stationary phase. The parameter  $m_{\text{RP}}$  characterizes the effect of the increasing concentration of water in the mobile phase upon the retention due to the RP mechanism in water rich-mobile phases, whereas the parameter  $m_{\text{HILIC}}$  is a measure of contribution of water to the decrease of retention in highly organic mobile phases (the HILIC range). A symbol  $a_2$  denotes an empirical system constant without special physical meaning. Jin *et al.* [35] have shown that Eq. (3) is more suitable for accurate calculation of the HILIC retention than polynomial empirical equations. However, Eq. (3) may fail at concentrations of water lower than 1-2 %.

The zwitterionic polymethacrylate BIGDMA-MEDSA columns show excellent stability and high efficiency (up to 70 000 theoretical plates  $\text{m}^{-1}$ ) providing dual retention mechanism for some polar compounds. In the present work, we investigated the effects of mobile phase composition and the dual mechanism on the retention, selectivity, and possibilities of separation of mixtures with barbiturates, sulfonamides, nucleosides and nucleic acid bases at the zwitterionic polymethacrylate BIGDMA-MEDSA micro-columns in the HILIC and the RP retention ranges.

## Experimental

Polyimide-coated fused silica capillaries (with i.d.: 320  $\mu\text{m}$ ) were obtained from J & W (Folsom, USA). 3-(trimethoxysilyl) propyl methacrylate, sodium hydroxide, hydrochloric acid, 1,4-butanediol, azobisisobutyronitrile and toluene were all purchased from Fluka. Uracil, phenol, thiourea, toluene, 1-propanol, *N,N*-dimethyl-*N*-metacryloxyethyl-*N*-(3-sulfopropyl)amonium betaine (MEDSA), bisphenol A glycerolate dimethacrylate (BIGDMA), ammonium acetate — all of highest purity grade — were obtained from Sigma–Aldrich in best available quality. Acetonitrile and tetrahydrofuran for gradient HPLC were from Merck. Distilled water was purified in a DEMIWA station (model 5ROI; Watek, Ledec nad Sázavou, the Czech Republic). The standard compounds listed in Fig. 2 were purchased from Sigma–Aldrich barbiturates (barbital, phenobarbital, pentobarbital, amobarbital, hexobarbital, and barbituric acid), sulfonamides (sulfadimidine, sulfanilamide, phthalazole, sulfaguanidine, sulfacetamide, and sulfathiazole), nucleosides and nucleic bases (adenine, thymine, cytosine, uracil, adenosine, guanosine, cytidine, 2-deoxyadenosine, and 2-deoxyguanosine).

In order to improve the stability of the polymethacrylate monolithic column

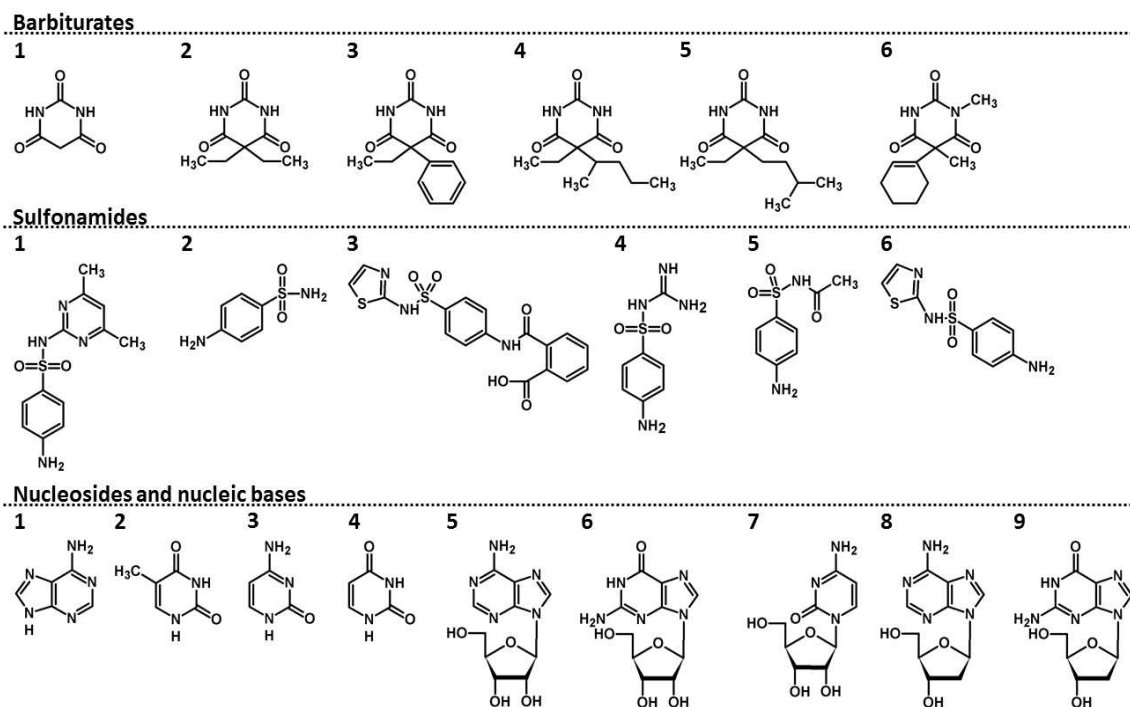


Fig. 2 Structures of analytes. Barbiturates: (1) barbituric acid, (2) barbital, (3) phenobarbital, (4) pentobarbital, (5) amobarbital, (6) hexobarbital; Sulfonamides: (1) sulfadimidine, (2) sulfanilamide, (3) phthalazole, (4) sulfaguanidine, (5) sulfacetamide, (6) sulfathiazole; Nucleosides and nucleic bases: (1) adenine, (2) thymine, (3) cytosine, (4) uracil, (5) adenosine, (6) guanosine, (7) cytidine, (8) 2-deoxyadenosine, (9) 2-deoxyguanosine

Table I Parameters  $a_1$ ,  $m_{RP}$  and  $m_{HILIC}$  of barbiturates of Eq. (3) on the BIGDMA-MEDSA column.  $id = 320 \mu\text{m}$ ,  $l = 174 \text{ mm}$ , coefficient of determination,  $D^2$ ,  $\varphi_{\min}$  (in %  $\text{vol} \times 10^{-2}$ ) volume fraction of water in the mobile phase at the HILIC-RP mode transition, Mobile phase: aqueous acetonitrile buffered with 10 mM ammonium acetate, 5-90 % water

	$a_1$	$m_{RP}$	$m_{HILIC}$	$RSC$	$D^2$	$\varphi_{\min}$
barbituric acid	$-3.94 \pm 0.04$	$3.88 \pm 0.05$	$4.76 \pm 0.05$	0.06	99.35	0.532
barbital	$-3.41 \pm 0.06$	$4.11 \pm 0.08$	$1.85 \pm 0.05$	0.84	97.27	0.195
phenobarbital	$-3.36 \pm 0.06$	$4.91 \pm 0.08$	$1.87 \pm 0.05$	0.82	97.99	0.165
pentobarbital	$-4.19 \pm 0.08$	$6.03 \pm 0.11$	$2.13 \pm 0.06$	1.52	97.65	0.153
amobarbital	$-4.52 \pm 0.13$	$6.40 \pm 0.18$	$2.25 \pm 0.09$	3.41	95.14	0.153
hexobarbital	$-3.67 \pm 0.06$	$5.45 \pm 0.08$	$1.67 \pm 0.05$	0.81	98.78	0.133

bed prior to *in-situ* polymerization, the fused silica capillaries were subsequently washed with acetone, water,  $0.2 \text{ mol l}^{-1}$  NaOH (all for 30 min), again with water to a neutral pH, then with  $0.2 \text{ mol l}^{-1}$  HCl for 30 min, and finally with ethanol. The



inner wall surface was activated by purging with 40% 3-(trimethoxysilyl) propyl methacrylate in 95% ethanol (with pH 5 adjusted with acetic acid) for 3 hours. The capillary was finally purged with ethanol, dried in a stream of nitrogen, and left at room temperature for 24 h before polymerization. Based on our earlier work [30], we employed polymerization mixtures containing zwitterionic sulfobetaine MEDSA functional monomer and bisphenol A glycerolate dimethacrylate BIGDMA as a cross-linking monomer. The monomers were dissolved in porogen solvents. The polymerization mixture contained 20 % *N,N*-dimethyl-*N*-methacryloxyethyl-*N*-(3-sulfopropyl) ammonium betaine (MEDSA), 15 % bisphenol A glycerolate dimethacrylate, 25 % 1,4-butanediol, 25 % 1-propanol, 15 % water and 1% azo-*bis*-isobutyronitrile initiator (with respect to the monomers). Fused-silica capillaries with modified internal walls were filled with the polymerization mixture, both ends of the capillaries sealed with rubber stoppers, and the capillaries kept for 20 h at 60 °C in a circulated-air thermostat. Following the polymerization reaction, both ends of each capillary were cut off, the capillary monolithic column was washed with acetonitrile, and finally with the mobile phase.

A modular micro-liquid chromatograph was assembled from:

- (a) a high-pressure gradient system including two LC10ADvp pumps and a gradient controller (Shimadzu; Kyoto, Japan);
- (b) a splitter QuickSplit™ valve, (Analytical Scientific Instruments; Richmond, USA)
- (c) a micro-valve injector with a 60 nL inner sample loop (Valco; Houston, USA) and an electronic time switch for injection of low-sample volumes;
- (d) a variable wavelength LCD 2083 UV detector with a silica capillary flow-through cell, (50 μm i.d.; ECOM, Prague, Czech Republic);
- (e) a personal computer with a chromatographic Clarity Data Station for Windows (Data Apex, Prague, the Czech Republic).

The capillary columns were connected to the injector and detector via zero-volume PTFE capillary units.

Stock solutions containing 1 mg ml<sup>-1</sup> of each solute were dissolved in the mobile phase and diluted to the concentrations yielding an adequate detector response. Sample volumes of 60 nl were injected in all experiments. Pre-mixed acetonitrile-water mobile phases buffered with 10 mM ammonium acetate were used in isocratic experiments, whereas buffered water and buffered acetonitrile were used as the components A and B in the gradient chromatography. All mobile phases were filtered through a Millipore 0.45 μm filter and degassed by sonication before use. Volumes of 60 nl sample were injected in all experiments. The mobile phase flow-rate was set in the range of 1-25 μ min<sup>-1</sup> as appropriate and being controlled using a stopwatch with a calibrated 100 μl microburette. The column hold-up volume,  $V_M$ , was determined as the elution volume of toluene in 95%

acetonitrile. All chromatographic experiments were performed at the laboratory temperature and repeated at least in triplicate. The retention times and the peak widths at the half peak height in mobile phases containing 5-95 % acetonitrile were evaluated using the Clarity Data Station evaluation software (Data Apex; Prague, the Czech Republic) and used for calculations of the retention volumes,  $V_R$ , retention factors,  $k = (V_R - V_M)/V_M$ , and other column characteristics.

## Results and Discussion

We investigated the effects of the composition of mobile phase on the retention and possibilities of separation of some polar compounds, the retention of which was earlier studied on particulate 2-hydroxyethyl methacrylate - ethanediol dimethacrylate copolymer gels and ion exchangers, namely barbiturates, sulfonamides [21], nucleic acid bases and nucleosides [20]. Figure 2 shows the structures of the sample compounds.

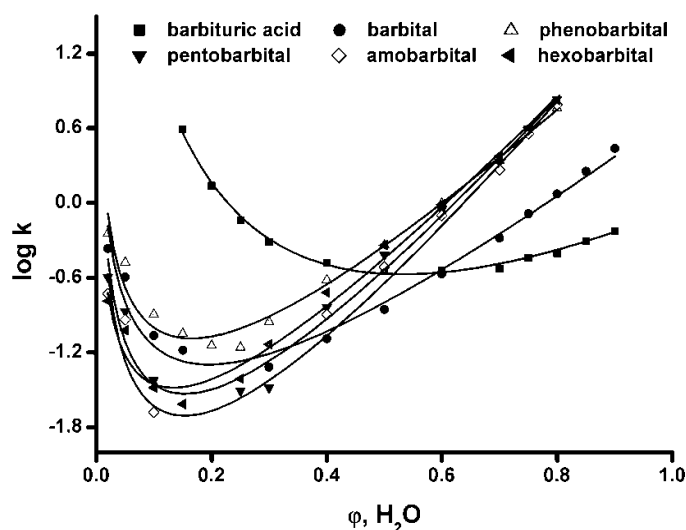


Fig. 3 Effect of the volume fraction of the water,  $\phi_{H_2O}$ , in buffered aqueous-organic mobile phases on the retention factors,  $k$ , of barbiturates on monolithic column BIGDMA-MEDSA. mobile phase (A): 10 mM  $NH_4Ac$  in water (pH = 3), mobile phase (B): 10 mM  $NH_4Ac$  in acetonitrile; mobile phase composition: 10-98 % mobile phase B

### Retention and Separation of Barbiturates at BIGDMA-MEDSA Columns

Barbiturates have been widely used as hypnotics, sedatives, and analgesics. Figure 3 shows the effect of the mobile phase composition on the retention of the six barbiturate standards (see Fig. 2 for structures), on a BIGDMA-MEDSA capillary

column. Barbituric acid (1) is the most polar and most retained substance in the HILIC mode (Fig. 3, left-hand part of the plot) and shows minimal retention in a buffered aqueous-organic mobile phase with 50 % water. The retention further does not increase significantly at higher concentrations of water, which illustrates a very low contribution of the hydrophobic interactions to the retention in the RP mobile phase range (see right-hand part of the plot).

Substituted barbiturates are less polar and markedly less retained at high acetonitrile concentrations (> 50 %) in comparison to barbituric acid (Fig. 3). Pheno-, pento-, amo-, and hexo-barbital have a very similar retention, both in the high (RP, right-hand part) and low (HILIC, left-hand part) retention range. The retention over the full-mobile phase composition range can be satisfactorily described by Eq. (3) — see constants  $a_1$ ,  $m_{RP}$ ,  $m_{HILIC}$  in Table I. The U-turn in retention is observed at  $\varphi_{min}$  corresponding to 13-20 % water in the mobile phase, much less than 53 % for barbituric acid. The molecule of barbital contains smaller hydrocarbon substituents and, as a consequence, it exhibits the lowest retention of all barbiturates at high water concentrations (in the RP retention range).

The mobile phase affects very significantly the selectivity of separation of barbiturates in buffered aqueous-organic mobile phases (Fig. 4). In 95% buffered acetonitrile, corresponding to the HILIC separation range, pentobarbital, amobarbital and hexobarbital with large non-polar substituents are not retained and co-elute in a single peak (Fig. 4a). Phenobarbital and barbital with smaller or more polar substituents could be partly resolved, even though they are retained relatively weakly. The phenyl substituent is more polar than the methyl group and hence, phenobarbital elutes later than barbital in 95% acetonitrile, where barbituric acid is retained very strongly. In 60% buffered acetonitrile (40 % aqueous component) the baseline separation of barbiturates was not achieved because of a very low retention, but the elution order could be determined: barbital - amobarbital - pentobarbital - hexobarbital - phenobarbital - barbituric acid (Fig. 4b). Obviously, both the HILIC and the reversed-phase interactions contribute to the retention. Fig. 4c shows the separation in 30% buffered acetonitrile, i.e., essentially in the reversed-phase mechanism range (70 % aqueous component). Here, the most polar barbituric acid elutes first, followed with barbital. The four remaining barbiturates are resolved only partly; especially, phenobarbital and pentobarbital co-elute. Such a behavior agrees with the mobile phase effects on retention shown in Fig. 3.

On the whole, the HILIC-mode mobile phase range is very narrow for successful separation of all barbiturates. The RP mode provides a higher retention, but low selectivity of separation, which allows one only partial separation. Probably, a combination of the HILIC and RP mechanism (like that in 70% buffered acetonitrile) could enable the fast separation and identification of all barbiturates when using a longer BIGDMA-MEDSA column.

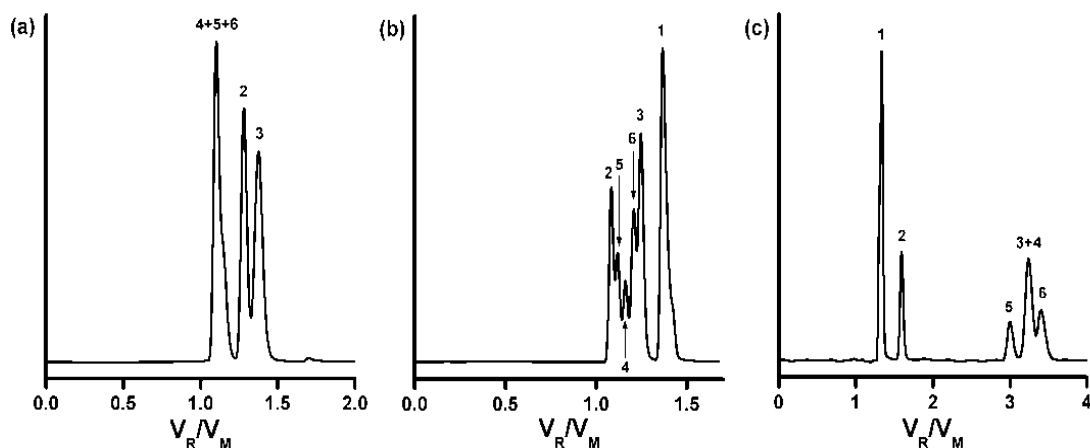


Fig. 4 Separation of barbiturates on column BIGDMA-MEDSA. (a) mobile phase: 95 % MF (A) and 5 % MF (B),  $F_m = 3.3 \mu\text{l min}^{-1}$ ,  $p = 1.9 \text{ MPa}$ ; (b) mobile phase: 60 % MF (A) and 40 % MF (B),  $F_m = 1.9 \mu\text{l min}^{-1}$ ,  $p = 4.1 \text{ MPa}$ ; (c) mobile phase: 30 % MF (A) and 70 % MF (B),  $F_m = 2.1 \mu\text{l min}^{-1}$ ,  $p = 5.0 \text{ MPa}$ ;  $L = 174 \text{ mm}$ ,  $\text{id} = 320 \mu\text{m}$ , UV detection at 214 nm; mobile phase (A): 10 mM  $\text{NH}_4\text{Ac}$  in water ( $\text{pH} = 3$ ); mobile phase (B): 10 mM  $\text{NH}_4\text{Ac}$  in acetonitrile sample: (1) barbituric acid, (2) barbital, (3) phenobarbital, (4) pentobarbital, (5) amobarbital, (6) hexobarbital

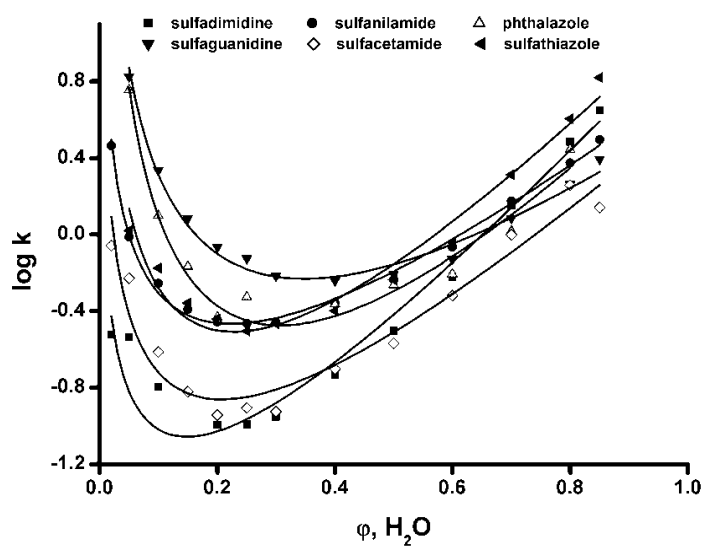


Fig. 5 Effect of the volume fraction of the water,  $\phi_{\text{H}_2\text{O}}$ , in aqueous-organic mobile phases on the retention factors,  $k$ , of sulfonamides on monolithic column BIGDMA-MEDSA. mobile phase (A): water ( $\text{pH} = 3$ ); mobile phase (B): acetonitrile; mobile phase composition: 15- 98 % mobile phase B

## Retention and Separation of Sulfonamides on BIGDMA-MEDSA Columns

Sulfonamides are antimicrobial agents derived from sulfanilamide, but largely differing in structures, whose predominant use is in veterinary medicine to treat or prevent infectious diseases. They are usually separated by the reversed-phase chromatography [36].

Figure 5 illustrates the effects of the volume fraction of water,  $\varphi_{\text{H}_2\text{O}}$ , over the full range composition of aqueous–organic mobile phases (15–98% acetonitrile) on the BIGDMA-MEDSA column on the retention and separation selectivity of six common sulfonamides (for their structures, see Fig. 2). The sulfonamides are retained both at high and low acetonitrile concentrations in the mobile phase, except for sulfacetamide (5) and sulfadimidine (1) that provide a low retention in mobile phases containing less than 20% acetonitrile. All sulfonamides are subject to the dual HILIC - RP retention mechanism, showing the U-turn concentration of aqueous component in the mobile phase,  $\varphi_{\text{min}}$  in between 15–35 %. However, sulfanilamide (2) and sulfathiazole (6) show a low selectivity of separation in the HILIC mode (Fig. 6a). The retention increases in the mobile phases containing 40 % and more aqueous mobile phase component (RP-mode). Sulfathiazole (6) is the most retained whereas sulfacetamide (5) is the compound with the weakest retention in the RP mode. Sulfadimidine (1) and phthalazole (3) show a low separation selectivity and co-elute in the RP mobile phase composition range (Fig. 6b). Table II lists the constants  $a_1$ ,  $m_{\text{RP}}$ ,  $m_{\text{HILIC}}$  of Eq. (3) obtained from the experimental data by non-linear regression, with the coefficient of variation in between 93.4 to 99.4 %. Phthalazole and sulfaguanidine provide the largest range of HILIC retention mode, up to 31 % and 35 % aqueous component, respectively.

Table II Parameters  $a_1$ ,  $m_{\text{RP}}$  and  $m_{\text{HILIC}}$  of sulfonamides of Eq. (3) on the BIGDMA-MEDSA column.  $i_d = 320 \mu\text{m}$ ,  $l = 167 \text{ mm}$ , coefficient of determination,  $D^2$ ,  $\varphi_{\text{min}}$  (in % vol $\times 10^{-2}$ ) volume fraction of water in the mobile phase at the HILIC-RP mode transition. Mobile phase: aqueous acetonitrile, 5–90 % water

	$a_1$	$m_{\text{RP}}$	$m_{\text{HILIC}}$	$RSC$	$D^2$	$\varphi_{\text{min}}$
sulfadimidine	$-2.66 \pm 0.05$	$3.72 \pm 0.07$	$1.27 \pm 0.04$	0.80	97.57	0.148
sulfanilamide	$-2.06 \pm 0.02$	$2.85 \pm 0.02$	$1.47 \pm 0.01$	0.07	99.39	0.224
phthalazole	$-3.24 \pm 0.05$	$4.13 \pm 0.07$	$2.92 \pm 0.05$	0.37	97.42	0.307
sulfaguanidine	$-2.32 \pm 0.04$	$2.92 \pm 0.05$	$2.34 \pm 0.03$	0.19	97.93	0.348
sulfacetamide	$-2.57 \pm 0.07$	$3.20 \pm 0.09$	$1.53 \pm 0.05$	1.09	93.41	0.208
sulfathiazole	$-2.67 \pm 0.06$	$3.82 \pm 0.08$	$2.01 \pm 0.06$	0.56	96.93	0.228

Five sulfonamides could be separated in the HILIC mode with 90% aqueous acetonitrile (Fig. 6a). The selectivity was not sufficient for the separation of sulfanilamide and sulfathiazole. Another group of five sulfonamides were partly separated in 40% aqueous acetonitrile (in the RP separation mode); sulfadimidine and phthalazole co-elute (Fig. 6b). On the whole, sulfonamides exhibit a complementary selectivity of separation in the HILIC and RP ranges. Table III reveals the relative retention of sulfonamides in the HILIC range (95 % ACN) to the RP range (20 % ACN),  $\alpha$ (HILIC/RP). Two more polar sulfonamides show higher retention in the HILIC mode, two less polar in the RP mode. By combining the information obtained from analysis in mobile phases with high and low acetonitrile concentrations, all sample compounds could be identified and determined.

Table III Retention factors of sulfonamides in mobile phase water and acetonitrile.  $k$ , retention factors in reversed-phase mode (related to uracil) and HILIC mode (related to toluene); relative retention in HILIC and RP mobile phase range. Selectivity,  $\alpha = k_{\text{HILIC}} / k_{\text{RP}} = k_{95\% \text{ACN}} / k_{20\% \text{ACN}}$

	Compound	Retention factor, $k$		Selectivity, $\alpha$
		20 % ACN	95 % ACN	
1	sulfadimidine	3.05	0.29	0.10
2	sulfanilamide	2.36	0.97	0.41
3	phthalazole	2.79	5.71	2.05
4	sulfaguanidine	1.83	6.70	3.67
5	sulfacetamide	1.81	0.59	0.33
6	sulfathiazole	4.02	1.05	0.26

### Retention and Separation of Nucleosides and Nucleic Bases on BIGDMA-MEDSA Column

Nucleosides and nucleic bases are often separated by HILIC HPLC. The BIGDMA-MEDSA column provides a higher retention of the nine nucleosides and bases tested within the low water concentration (HILIC) range, in comparison to the RP separation mode (Fig. 7). The four-parameter equation, Eq. (5) describes appropriately the retention, with the coefficients of variation in the range 98.3 %-99.1 % (Table IV).

Nucleosides and nucleic bases are strongly retained in the mobile phases with low water content. An increasing proportion of water in the mobile phase

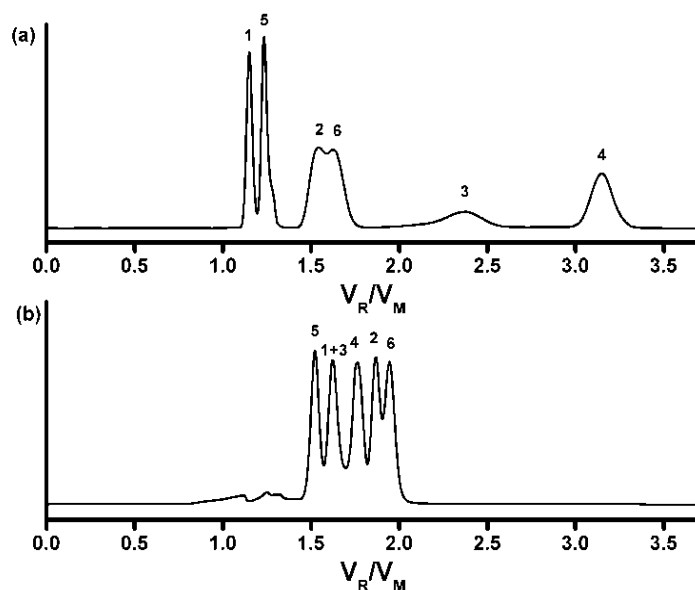


Fig. 6 Separation of sulfonamides on column BIGDMA-MEDSA. (a) mobile phase: 90 % acetonitrile,  $F_m = 4.2 \mu\text{l min}^{-1}$ ,  $p = 2.9 \text{ MPa}$ ; (b) mobile phase: 40 % acetonitrile,  $F_m = 3.6 \mu\text{l min}^{-1}$ ,  $p = 8.1 \text{ MPa}$ ;  $L = 167 \text{ mm}$ ,  $\text{id} = 320 \mu\text{m}$ , UV detection at 214 nm; mobile phase (A): water, mobile phase (B): acetonitrile sample: (1) sulfadimidine, (2) sulfanilamide, (3) phthalazole, (4) sulfaguanidine, (5) sulfacetamide, (6) sulfathiazole

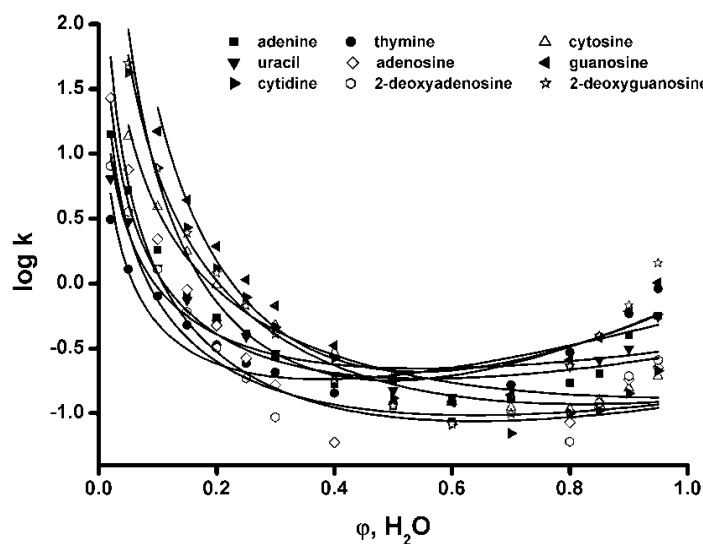


Fig. 7 Effect of the volume fraction of the water,  $\phi_{\text{H}_2\text{O}}$ , in buffered aqueous-organic mobile phases on the retention factors,  $k$ , of nucleosides and nucleic bases on monolithic column BIGDMA-MEDSA. mobile phase (A): 10 mM  $\text{NH}_4\text{Ac}$  in water ( $\text{pH} = 3$ ); mobile phase (B): 10 mM  $\text{NH}_4\text{Ac}$  in acetonitrile; mobile phase composition: 5-98 % mobile phase B

Table IV Parameters  $a_1$ ,  $m_{RP}$  a  $m_{HILIC}$  of nucleosides and nucleic bases of Eq. (5) on a BIGDMA-MEDSA column.  $id = 320 \mu\text{m}$ ,  $l = 166 \text{ mm}$ , coefficient of determination,  $D^2$ ,  $\varphi_{\min}$  (in  $\% \text{ vol} \times 10^{-2}$ ) volume fraction of water in the mobile phase at the HILIC-RP mode transition., mobile phase: aqueous acetonitrile buffered with 10 mM ammonium acetate, 5-90 % water

Compound	$a_1$	$m_{RP}$	$m_{HILIC}$	
adenine	$1.22 \pm 0.03$	$12.68 \pm 1.69$	$36.41 \pm 8.65$	
thymin	$0.50 \pm 0.02$	$19.85 \pm 3.04$	$93.14 \pm 27.79$	
cytosine	$1.63 \pm 0.05$	$4.07 \pm 0.45$	$8.83 \pm 1.26$	
uracil	$0.89 \pm 0.02$	$8.07 \pm 0.78$	$19.86 \pm 3.33$	
adenosine	$1.50 \pm 0.04$	$39.25 \pm 11.11$	$231.00 \pm 123.54$	
guanosine	$1.95 \pm 0.04$	$133.78 \pm 92.19$	$2.76 \times 10^3 \pm 3.77 \times 10^3$	
cytidine	$2.22 \pm 0.06$	$7.53 \pm 0.82$	$17.04 \pm 2.72$	
2-deoxyadenosine	$1.09 \pm 0.03$	$69.97 \pm 26.79$	$740.61 \pm 551.32$	
2-deoxyguanosine	$2.15 \pm 0.05$	$32.55 \pm 5.59$	$145.29 \pm 47.45$	
Compound	$b$	$RSC$	$D^2$	$\varphi_{\min}$
adenine	$1.43 \pm 0.26$	0.61	98.27	0.547
thymin	$0.65 \pm 0.12$	0.20	98.67	0.498
cytosine	$4.35 \pm 0.74$	0.34	99.11	0.712
uracil	$1.90 \pm 0.27$	0.26	98.76	0.542
adenosine	$0.51 \pm 0.16$	1.13	98.42	0.593
guanosine	$0.12 \pm 0.09$	0.27	99.19	0.718
cytidine	$3.10 \pm 0.51$	0.63	99.01	0.660
2-deoxyadenosine	$0.25 \pm 0.10$	0.63	98.71	0.594
2-deoxyguanosine	$0.72 \pm 0.16$	0.77	98.61	0.548

results in the decrease of retention down to minimum, which is observed at  $\varphi_{\min} = 0.498$  for thymine, which is the substance with the weakest retention. On the other hand, guanosine provides the broadest water concentration range of the HILIC separation mode, with the transition-mode water volume fraction  $\varphi_{\min} = 0.718$  (Table IV), close to the  $\varphi_{\min} = 0.712$  for cytosine. The retention order increases in a row of thymine, uracil, 2-deoxyadenosine, adenine, adenosine, cytosine, 2-deoxyguanosine, cytidine, and guanosine (Fig. 7).

Table V lists the selectivity coefficients,  $\alpha$ , of nucleosides and bases as the ration of the retention factors,  $k$ , in the HILIC (90% ACN) versus the RP mode



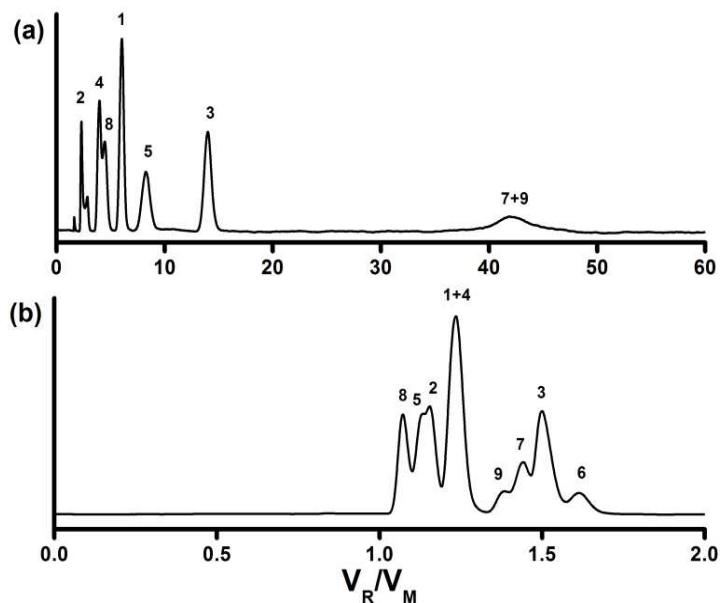


Fig. 8 Separation of nucleosides and nucleic bases on BIGDMA-MEDSA column. (a) mobile phase: 95 % acetonitrile,  $F_m = 14.3 \mu\text{l min}^{-1}$ ,  $p = 6.6 \text{ MPa}$ ; (b) mobile phase: 70 % acetonitrile,  $F_m = 2.0 \mu\text{l min}^{-1}$ ,  $p = 3.6 \text{ MPa}$ ;  $L = 166 \text{ mm}$ ,  $\text{id} = 320 \mu\text{m}$ , UV detection at 214 nm; mobile phase (A): 10 mM  $\text{NH}_4\text{Ac}$  in water ( $\text{pH} = 3$ ); mobile phase (B): 10 mM  $\text{NH}_4\text{Ac}$  in acetonitrile; sample: (1) adenine, (2) thymine, (3) cytosine, (4) uracil, (5) adenosine, (6) guanosine, (7) cytidine, (8) 2-deoxyadenosine, (9) 2-deoxyguanosine

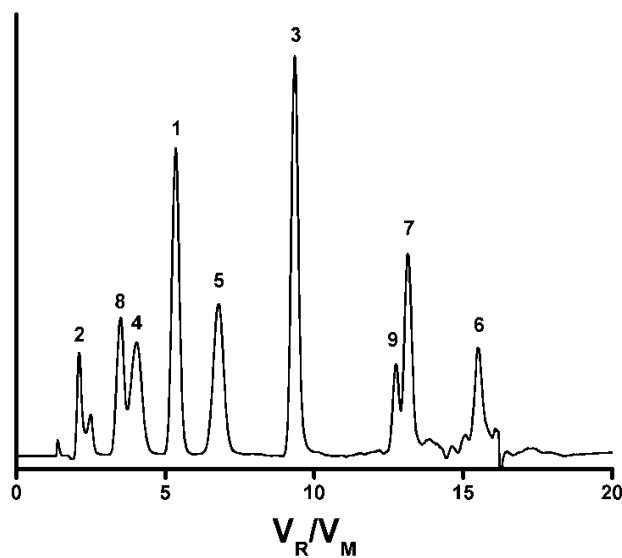


Fig. 9 Gradient separation of nucleosides and nucleic bases on BIGDMA-MEDSA column.  $L = 166 \text{ mm}$ ,  $\text{id} = 320 \mu\text{m}$ ,  $F_m = 10.9 \mu\text{l min}^{-1}$ ,  $p = 4.2 \text{ MPa}$ , UV detection at  $\lambda = 214 \text{ nm}$ ; mobile phase (A): 10 mM  $\text{NH}_4\text{Ac}$  in water ( $\text{pH} = 3$ ); mobile phase (B): 10 mM  $\text{NH}_4\text{Ac}$  in acetonitrile; gradient of mobile phase: 0 min – 95 % MF (B), 15 min – 80 % MF (B); sample: (1) adenine, (2) thymine, (3) cytosine, (4) uracil, (5) adenosine, (6) guanosine, (7) cytidine, (8) 2-deoxyadenosine, (9) 2-deoxyguanosine

Table V Retention factors of nucleosides and bases in mobile phase water and acetonitrile.  $k$ , retention factors in reversed-phase mode (related to uracil) and HILIC mode (related to toluene); relative retention in HILIC and RP mobile phase range, Selectivity,  $\alpha = k_{\text{HILIC}} / k_{\text{HP}} = k_{95\% \text{ACN}} / k_{20\% \text{ACN}}$

	Compound	Retention factor, $k$		Selectivity, $\alpha$
		5 % ACN	90 % ACN	
1	adenine	0.56	1.82	3.22
2	thymine	0.91	0.80	0.88
3	cytosine	0.19	3.90	20.10
4	uracil	0.56	1.32	2.37
5	adenosine	0.22	2.20	9.79
6	guanosine	1.01	14.87	14.73
7	cytidine	0.21	7.76	36.50
8	2-deoxyadenosine	0.26	1.28	4.99
9	2-deoxyguanosine	1.43	7.72	5.39

(5% ACN). The data clearly demonstrate significantly higher selectivity of the column for the acetonitrile-rich mobile phase in the HILIC mode. In 95% buffered aqueous acetonitrile, the nucleosides and nucleic bases elute in the order: thymine, uracil, 2-deoxyadenosine, adenine, adenosine, and cytosine, followed by cytidine and 2-deoxyguanosine that co-elute under these conditions in the HILIC separation mode (Fig. 8a). Guanosine is strongly retained under HILIC conditions and does not elute in 95% buffered aqueous acetonitrile. Figure 8b then documents the separation in 70% buffered aqueous acetonitrile, where the sample elutes in the order: 2-deoxyadenosine, adenosine, thymine, adenine-uracil, 2-deoxyguanosine, cytidine, and cytosine.

Satisfactory separation of all tested nucleosides and bases was achieved using a gradient with the decreasing acetonitrile concentration, from the initial 95% decreasing to 80% buffered aqueous acetonitrile.

All compounds were separated in 15 minutes, including cytidine and 2-deoxyguanosine that could not be separated under isocratic conditions. Finally, also guanosine eluted from the column; see Fig. 9.

## Conclusion

The new BIGDMA-MEDSA polymethacrylate zwitterionic monolithic micro-columns can be used for separation of various classes of polar samples, including

barbiturates, sulfonamides, nucleic bases, and nucleosides; however, within different retention ranges of the buffered aqueous acetonitrile. For the proper separation, two retention modes, HILIC and RP, can be combined using a single BIGDMA-MEDSA column depending on the sample character: the HILIC mode in mobile phases with high concentrations of acetonitrile in buffered aqueous-organic mobile phases, whereas the RP mode is applicable in more aqueous media.

Furthermore, the two separation modes can be used for the same column, with a short re-equilibration period (for 10 min) between the subsequent injections in the HILIC and in the RP mobile phases. This alternating approach with the BIGDMA-MEDSA in the first dimension was used for comprehensive two-dimensional LC-LC separation of polyphenolic compounds and flavonoids, combined with the reversed-phase separation on a short (5 cm) octadecyl silica superficially porous or monolithic column in the second dimension [36].

## Acknowledgement

*This work was supported by the Czech Science Foundation, project No. P206/12/0398.*

## References

- [1] Svec F.: *J. Chromatogr. A*, **1228**, 250 (2012).
- [2] Minakuchi H., Nakanishi K., Soga N., Ishizuka N., Tanaka N.: *Anal. Chem.* **68**, 3498 (1996).
- [3] Hjertén S., Liao J., Zhang R.: *J. Chromatogr.* **473**, 273 (1989).
- [4] Svec F., Fréchet J.M.J.: *Anal. Chem.* **64**, 820 (1992).
- [5] Svec F.: *J. Sep. Sci.* **27**, 747 (2004).
- [6] Svec F.: *J. Chromatogr. A* **1217**, 902 (2010).
- [7] Urban J., Svec F., Fréchet J.M.J.: *J. Chromatogr. A* **1217**, 8212 (2010).
- [8] Nischang I., Teasdale I., Bruggemann O.: *J. Chromatogr. A* **1217**, 7514 (2010).
- [9] Nischang I., Teasdale I., Bruggemann O.: *Anal. Bioanal. Chem.* **400**, 2289 (2011).
- [10] Urban J., Jandera P.: *Anal. Bioanal. Chem.* **405**, 2123 (2013).
- [11] Currivan S., Jandera P.: *Chromatography* **1**, 24 (2014).
- [12] Jandera P., Staňková M., Škeříková V., Urban J.: *J. Chromatogr. A* **1274**, 97 (2013).
- [13] Alpert A.J.: *J. Chromatogr.* **499**, 177 (1990).
- [14] Jandera P.: *Anal. Chim. Acta* **692**, 1 (2011).
- [15] Moravcová D., Planeta J., Kahle V., Roth M.: *J. Chromatogr. A* **1270**, 178

- (2012).
- [16] Xu M., Peterson D.S., Rohr T., Svec F., Fréchet J.M.J.: *Anal. Chem.* **75**, 1011 (2003).
- [17] Que A.H., Konse T., Baker A.G., Novotny M.V.: *Anal. Chem.* **72**, 2703 (2000).
- [18] Que A.H., Novotny M.V.: *Anal. Chem.* **74**, 5184 (2002).
- [19] Guerrouache M., Pantazaki A., Millot M.C., Carbonnier B.: *J. Sep. Sci.* **33**, 787 (2010).
- [20] Jandera P., Churáček J., Čáslavský J., Vojáčková M.: *Chromatographia* **13**, 734 (1980).
- [21] Jandera P., Churáček J., Szabó D.: *Chromatographia* **14**, 7 (1981).
- [22] Jandera P., Churáček J., Čáslavský J., Szabó D.: *Chromatographia* **14**, 100 (1981).
- [23] Holdšvendová P., Suchánková J., Bunčec M., Bačkovská V., Coufal P.: *J. Biochem. Biophys. Methods* **70**, 23 (2007).
- [24] Foo H.C., Heaton J., Smith N.W., Stanley S.: *Talanta* **100**, 344 (2012).
- [25] Viklund C., Irgum K.: *Macromolecules* **33**, 2539 (2000).
- [26] Vicklund C., Sjorgen A., Irgum K., Nes I.: *Anal. Chem.* **73**, 444 (2001).
- [27] Jiang Z., Smith N.W., Ferguson P.D., Taylor M.R.: *Anal. Chem.* **79**, 1243 (2007).
- [28] Urban J., Škeříková V., Jandera P., Kubičková R., Pospíšilová M.: *J. Sep. Sci.* **32**, 2530 (2009).
- [29] Lin H., Ou J., Zhang Z., Dong J., Wu M., Zou H.: *Anal. Chem.* **84**, 2721 (2012).
- [30] Staňková M., Jandera P., Škeříková V., Urban J.: *J. Chromatogr. A* **1289**, 47 (2013).
- [31] Jandera P., Staňková M., Hájek T.: *J. Sep. Sci.* **36**, 2430 (2013).
- [32] Snyder L.R., Dolan J.W., Gant J.R.: *J. Chromatogr.* **165**, 3 (1979).
- [33] Jandera P., Churáček J., Svoboda L.: *J. Chromatogr.* **174**, 35 (1979).
- [34] Jandera P.: *J. Separation Sci.* **31**, 1421 (2008).
- [35] Jin G., Guo Z., Zhang F., Xue X., Jin Y., Liang X.: *Talanta* **76**, 522 (2008).
- [36] Hájek T., Jandera P., Staňková M., Česla P.: *J. Chromatogr. A* **1446**, 91 (2016).